



HAL
open science

Influence of stabilizers on the microstructure of fresh sorbets: X-ray micro-computed tomography, cryo-SEM, and Focused Beam Reflectance Measurement analyses

Véronique Masselot, Véronique Bosc, Hayat H. Benkhelifa

► To cite this version:

Véronique Masselot, Véronique Bosc, Hayat H. Benkhelifa. Influence of stabilizers on the microstructure of fresh sorbets: X-ray micro-computed tomography, cryo-SEM, and Focused Beam Reflectance Measurement analyses. *Journal of Food Engineering*, 2021, 300, pp.110522. 10.1016/j.jfoodeng.2021.110522 . hal-03265275

HAL Id: hal-03265275

<https://hal.science/hal-03265275>

Submitted on 6 Dec 2022

HAL is a multi-disciplinary open access archive for the deposit and dissemination of scientific research documents, whether they are published or not. The documents may come from teaching and research institutions in France or abroad, or from public or private research centers.

L'archive ouverte pluridisciplinaire **HAL**, est destinée au dépôt et à la diffusion de documents scientifiques de niveau recherche, publiés ou non, émanant des établissements d'enseignement et de recherche français ou étrangers, des laboratoires publics ou privés.

1 Influence of stabilizers on the microstructure of fresh sorbets: X-ray 2 micro-computed tomography, cryo-SEM, and FBRM analyses

3 Véronique Masselot^{a, b}, Véronique Bosc^b, Hayat Benkhelifa^{a, b}

4 ^aUniversité Paris-Saclay, INRAE, FRISE, 92761, Antony, France

5 ^bUniversité Paris-Saclay, INRAE, AgroParisTech, SayFood, 91300, Massy, France

6 Authors e-mail addresses: veronique.masselot@agroparistech.fr ; veronique.bosc@agroparistech.fr

7 Corresponding author: Hayat Benkhelifa. hayat.benkhelifa@agroparistech.fr. 16 rue Claude Bernard,
8 75231, Paris, France.

9 **Abstract**

10 X-ray micro-computed tomography was applied to determine the influence of stabilizers on
11 the microstructure of fresh sorbets (i.e. at the outlet of a batch freezer), and more particularly
12 on the air phase and the ice phase. Sucrose sorbets were tested with addition of one stabilizer:
13 locust bean gum (LBG), hydroxypropylmethylcellulose (HPMC) or carboxymethylcellulose
14 (CMC). It was shown that HPMC increased the quantity and decreased the size of air bubbles;
15 it also decreased the ice crystals size unlike other stabilizers which had no effect on the size of
16 ice crystals. Results were successfully compared with data from Cryo-Scanning Electron
17 Microscopy and completed with Focused Beam Reflectance Measurement analyses applied
18 for dynamic studies during freezing process. The effect of HPMC on the ice phase would be
19 linked to its surfactant properties; air bubbles could prevent crystal growth during the freezing
20 process.

21 **Keywords**

22 Fresh sorbet ; Microstructure ; stabilizers ; X-ray micro-computed tomography ; ice crystal
23 size ; air bubble size.

24 **1. Introduction**

25 Sorbet is a triphasic frozen system, consisting of ice crystals and air bubbles dispersed in an
26 unfrozen matrix highly concentrated with sugars and stabilizers. Before freezing, the mix (i.e.
27 the mixture of ingredients) is composed of about 70%wt of water, almost 30%wt of sugars
28 (sugars naturally occurring in fruits and added sugars) and up to 0.5%wt of stabilizers

29 (Arbuckle, 1986; Clarke, 2012; Marshall and Arbuckle, 1996; Marshall et al., 2003; Stogo,
30 1998). The freezing step takes place in a scraped surface heat exchanger (SSHE) or freezer.
31 The mix is introduced at about 4 °C and when it touches the cold walls of the exchanger, a
32 layer of ice is immediately formed. Rotating scraper blades scrape off the ice crystals and
33 disperse them throughout the product which is increasingly enriched with ice. Air is
34 introduced at the same time. The unfrozen residual solution concentrates in sugar and
35 stabilizing throughout the freezing; its viscosity increases. At the outlet of the exchanger, the
36 sorbet temperature is about -6 °C and contains about 40% of ice; the concentration of sugars
37 and stabilizers in the unfrozen matrix is almost double that in the original mix. In the case of
38 sorbets, air can occupy up to 30% of the volume (Marshall et al., 2003). Sorbets are consumed
39 at frozen state, so their sensory properties are strongly dependent on ice crystals properties
40 (i.e. number and size). Controlling the amount and the size of air bubbles is another important
41 factor as air has also a significant influence on the textural properties of the finished product
42 (Clarke, 2012; Goff and Hartel, 2013).

43 The stabilizers usually found in the formulation of sorbets are natural polysaccharides such as
44 seed gums: guar gum (GG) and locust bean gum (LBG); cellulose derivatives:
45 carboxymethylcellulose (CMC) and hydroxypropylmethylcellulose (HPMC); and microbial
46 gum: xanthan gum (XG) (Thombare et al., 2016). Although their rheological properties have
47 been rarely studied in sugar solutions and at temperatures below zero, it is known that their
48 presence greatly increases the viscosity of the mix and of the residual unfrozen solution (Goff
49 et al., 1993; Masselot et al., 2020a). Some stabilizers solutions also develop elastic properties
50 under these conditions (Doyle et al., 2006; Masselot et al., 2020a; Patmore et al., 2003).
51 Although the mechanisms involved are not fully described, the increase in viscosity or the
52 appearance of viscoelastic or even gelling properties due to stabilizers could influence
53 crystallization by affecting the diffusion of molecules or heat transfers (Blond, 1988; Goff et
54 al., 1999; Goff and Hartel, 2013; Muhr and Blanshard, 1986). Some stabilizers, such as
55 HPMC, are also known for their surfactant properties, they facilitates the incorporation of air
56 and stabilizes the formed foam by slowing down the coalescence of air bubbles (Clarke, 2012;
57 Sarkar, 1984). A higher quantity of air due to stabilizers could also influence crystallization;
58 air bubbles could cause mechanical hindrance and lead to smaller ice crystals (Clarke, 2012;
59 Flores and Goff, 1999; Thomas, 1981).

60 The influence of stabilizers on crystallization in sorbets is still a subject of debate in the
61 literature; results seem to depend on the type of polymer, on the freezing process and the

62 analysis technique applied. Furthermore, most of the studies were carried out after a storage
63 step at temperatures well below the outlet temperature of an SSHE. It is therefore difficult to
64 conclude about the influence of stabilizers on the initial microstructure of the analyzed
65 products. Finally, the mechanisms involved are rarely mentioned by the authors. Fernandez et
66 al. (2007) studied the influence of the addition of 0.3% of stabilizers on the ice crystals size in
67 16% sucrose solutions frozen using a batch High Pressure Assisted Freezing (HPAF) process.
68 The authors found that guar gum gave larger crystals compared to an unstabilized sample,
69 whereas the addition of an equimolar mixture of xanthan and LBG gave smaller crystals. This
70 result was explained by the ability of the xanthan / LBG blend to form a gel which would
71 decrease molecular mobility required for crystallization. Flores and Goff (1999) found that the
72 addition of 0.6% of CMC, guar gum or xanthan gum to a 26% sucrose solution did not
73 influence ice crystals size. The authors used a batch SSHE.

74 Regarding air bubbles, Chang and Hartel (2002) studied the effect of adding up to 0.5% of a
75 blend containing carrageenans, guar and CMC on the aeration of an ice cream frozen in a
76 batch freezer. The blend did not affect the quantity of air introduced in the ice cream
77 (overrun). Stabilizers decreased the size of bubbles during the beginning of the freezing
78 process, while after 6 minutes, the bubbles were about the same size regardless of the sample.
79 This result was attributed to the evolution in apparent viscosity of sorbets: at the start of
80 freezing the stabilized mixes were significantly more viscous than the control sample whereas
81 all the finished products had the same apparent viscosity. This study focused on ice creams
82 containing fat and emulsifiers; then it is difficult to conclude about the specific effect of
83 stabilizers on the aeration of sorbets; that was not studied in the literature.

84 Studies cited above were performed using microscopic techniques: cryo-Scanning Electron
85 Microscopy (SEM) or optical microscopy. Although they are powerful and allow observations
86 with high resolutions, quantitative analysis is difficult : results are greatly dependent on the
87 visualized plane since the whole sample cannot be analyzed, and since samples are visualized
88 in 2 dimensions, a large number of particles has to be analyzed to ensure that results are
89 statistically representative (Hernández-Parra et al., 2018). 3D imaging techniques offer the
90 possibility of observing the entire sample in three dimensions, thus quantitative analysis is
91 greatly simplified and more reliable compared to the 2D techniques mentioned above. In
92 particular, X-ray micro-computed tomography (X-ray micro-CT) is well adapted to the typical
93 size of the frozen food microstructures (above 100 μm). This technique can be non-invasive
94 and non-destructive; several authors have successfully analyzed frozen food products directly

95 at the frozen state (Mulot et al., 2019; Vicent et al., 2019; Vicent et al., 2017). However, most
96 of the studies about the microstructure of frozen foods applied micro-CT at ambient
97 temperature coupled with a destructive freeze drying step (Kobayashi et al., 2014; Mousavi et
98 al., 2005; Mousavi et al., 2007; Ullah et al., 2014; Zhao and Takhar, 2017). In the case of
99 sorbets, freeze drying is not relevant, since the product would be totally melted; therefore the
100 sample has to be observed directly at frozen state.

101 The influence of stabilizers on the size and morphology of ice crystals or air bubbles in
102 sorbets has not been studied using X-ray micro-CT; most studies dedicated to frozen desserts
103 using micro-CT deals with the effect of storage periods on the microstructure of ice creams
104 (Guo et al., 2018; Guo et al., 2017; Mo et al., 2019; Mo et al., 2018; Pinzer et al., 2012). A
105 better understanding of the mechanisms that take place during the storage of ice cream was
106 obtained in these studies, where recrystallization and coalescence of air bubbles occur due to
107 temperature changes. Their authors developed powerful and complex tools to maintain
108 samples at frozen state and at temperatures far below the temperature encountered at the exit
109 of a freezer. Masselot et al. (2020b) recently described a methodology to study the
110 microstructure of fresh frozen sorbets at the freezer exit temperature of about -6 °C using X-
111 ray micro-CT device. Applying such a tool to sorbets of several compositions is an
112 unprecedented challenge; it would allow identifying the influence of the formulation on the
113 establishment of the microstructure before the product evolves during storage.

114 The dynamic analysis of the size of ice crystals during the freezing process would complete
115 the observation made at the end of the process; it would allow a better understanding of the
116 dynamics of crystallization and of effects of stabilizers during freezing. This study can be
117 performed using Focused Beam Reflectance Measurement (FBRM), which is a real time
118 method based on light backscattering to evaluate sizes of solid particles such as ice crystals.
119 Although data collected are chord lengths and not diameters, this technique makes it possible
120 to observe trends in the evolution of particle size. FBRM was successfully applied to the
121 dynamic analysis of the freezing of sugar/water solutions or commercial sorbet mixes
122 containing stabilizers (Arellano et al., 2012; Arellano et al., 2011; Haddad Amamou et al.,
123 2010). However, no publication deals with the influence of stabilizers on the crystallization of
124 sorbets using FBRM.

125 The objective of the present study was to determine the effect of several stabilizers on the
126 establishment of the microstructure of a sorbet. Sorbet mixes containing water, sucrose and

127 one stabilizer (HPMC or CMC or LBG) were formulated and frozen in a batch freezer. Fresh
128 samples were analyzed using X-ray micro-CT directly after the freezing step. Images were
129 processed, ice crystals and air bubbles size distributions and volume or mass fractions were
130 obtained. Results were compared and successfully confirmed thanks to cryo-SEM analyzes. In
131 order to better understand the dynamics of the mechanisms of crystallization, the study was
132 completed with a real-time analysis of freezing using an FBRM probe.

133 **2. Materials and methods**

134 **2.1.Preparation and freezing of sorbet mixes**

135 LBG was obtained from Cargill® (Viscogum™ FA 150); its viscosity at 1% in water was
136 evaluated by Cargill® between 2500 and 3000 mPa.s. HPMC was purchased from Dow®
137 (Methocel™ K4M), they evaluated its viscosity at about 4000 mPa.s (2% at 20 °C). It
138 contains 19 - 24% of methoxy groups and 7 – 12% of hydroxypropyl groups. Sodium CMC
139 was also obtained from Dow® (Walocel™ CRT 20000 PA) with a viscosity evaluated
140 between 1900 and 2600 mPa.s (1% in water at 25 °C). Its degree of substitution was between
141 70% and 95%. Sucrose was purchased from Béghin Say™. Solutions were prepared with
142 deionized water (conductivity 17 $\mu\text{S}\cdot\text{m}^{-1}$) to ensure constant quality of water.

143 The initial sugar concentration was set at 25%wt to represent that of an industrial sorbet mix
144 (Clarke, 2012; Goff and Hartel, 2013). Stabilizers were studied individually. The
145 concentrations of stabilizers were chosen so that the apparent viscosity of the mixes was equal
146 to that of a commercial sorbet mix (Lemon sorbet mix from La Laiterie de Montaigu,
147 Montaigu, France) containing a blend of three stabilizers (HPMC, LBG and guar gum) at the
148 beginning of the freezing step in a SSHE. Apparent viscosities were established at -1.5 °C
149 (i.e. temperature close to that of the sorbet at the beginning of the freezing process). The shear
150 rate (420 s^{-1}) corresponded to the shear rate at 1mm of the wall of the freezer; it was
151 determined using the analogy with a power-law fluid in a concentric cylinder viscometer
152 (Masselot et al., 2020a). The compositions of the mixes and their initial apparent viscosities
153 are shown in Table 1. A mix containing 0.3% of CMC was also formulated to be close to the
154 concentration usually encountered in commercial mixes.

155 Mixes were obtained by dispersing the mixture of sucrose and stabilizer in water at ambient
156 temperature using a magnetic stirrer. The solutions were then cooled for at least 12 hours at 4
157 °C before freezing to ensure the complete dissolution of polymers in the solvent (Clarke,

158 2012). In order to improve the contrast between the ice phase and the unfrozen residual
 159 solution during micro-CT imaging (Massetot et al., 2020b; Pinzer et al., 2012), 30g of sodium
 160 iodide (Na-I purchased from Merck®, CAS Number 7681-82-5) per kilogram of mix was
 161 added to the mixes just before the freezing step.

Table 1 : Compositions and apparent viscosities of the mixes

	Control	HPMC	LBG	CMC	
[Stabilizer] (%wt)	0	0.315	0.375	0.135	0.3
[Sucrose] (%wt)	25	25	25	25	25
Apparent viscosity at 420 s ⁻¹ and -1.5 °C (mPa.s)	5	40	40	40	80

162 Mixes (800 ml) were frozen in a batch domestic freezer (Magimix® Gelato Expert), the tank
 163 was 17 cm in diameter and contained two scrapping blades rotating at about 50 rpm. The
 164 temperature of the mixture was followed during freezing with a penetration thermometer
 165 (accuracy 0.5 °C, Testo 104, Testo, Forbach, France). Freezing was stopped at -6 °C
 166 corresponding to classical temperatures encountered for sorbets at the outlet of an industrial
 167 SSHE.

168 2.2.X-ray micro-CT analyses

169 Once the desired temperature in the freezer was reached, a plastic straw (6 mm of diameter,
 170 2.3 cm long) was inserted in the center of the freezer to extract a small quantity of fresh
 171 frozen sorbet. To ensure that the temperature of the sorbet was maintained at about -6 °C
 172 during the tomographic analysis, the frozen samples were placed in a specific thermostated
 173 box designed and manufactured in the laboratory, as described by Masselot et al. (2020b). The
 174 thermostated box and the plastic straw were stored in a freezer at -10 °C before the sampling
 175 of sorbet.

176 Samples were positioned in the X-ray micro-CT (DeskTom 130®, RX Solution, Chavanod,
 177 France); the system was operating at a X-ray tube voltage of 50 kV and a current intensity of
 178 160 µA. The acquisition time was short (12 minutes) to ensure that the temperature of the
 179 sorbet did not exceed -6°C (Massetot et al., 2020b). The resulting voxel resolution was 9 µm.
 180 XAct 2® software (RX Solution, Chavanod, France) was used to reconstruct the 3D volume
 181 from raw images using a filtered back-projection algorithm and applying a ring artifact filter.

182 More than 1300 slices were provided in 16-bits resolution from this volume reconstruction
183 (i.e. grayscale levels from 0 to 65536).

184 **2.3. Image processing and analysis of micro-CT data**

185 Slices were loaded on Avizo 2019.1® software (Thermo Fisher Scientific, Waltham, USA)
186 for image analysis. A cubic sub-volume (equivalent to 360 x 360 x 360 voxels equivalent to a
187 3.2 mm side cube) larger than the Representative Elementary Volume (Vicent et al., 2017)
188 was cropped at the center of the reconstructed 3D volume. The sorbets studied were triphasic
189 (i.e. air, ice and unfrozen matrix), thus images revealed three main materials with different
190 gray levels. Images were analyzed according to the methods described by Masselot et al.
191 (2020b) : watershed algorithms were applied to separate objects (i.e. ice crystals or air
192 bubbles) in contact with each other and a borderkill algorithm was used to suppress objects in
193 contact with the sub-volume walls. The remaining particles were labeled and individually
194 color-rendered. A 3D visualization of the particles was obtained.

195 Avizo® software allowed obtaining the volume fractions of the two phases and calculating
196 the equivalent diameter (i.e. diameter of a sphere having the same volume than the particle) of
197 each particle with equation 1.

$$198 \quad d_V = \sqrt[3]{\frac{6V}{\pi}} \quad (\text{Équation 1})$$

199 where V is the volume of the particle. The resolution limit of micro-CT analysis is commonly
200 assumed to be between two and three voxels size (Pinzer et al., 2012), in the case of the
201 present study this corresponded to particles having equivalent diameters larger than 20 µm
202 Therefore objects smaller than 20 µm were excluded from the quantitative analysis.

203 The volume fraction of ice without air φ_i was calculated according to equation 2.

$$204 \quad \varphi_i = \frac{V_{i0}}{V_{i0} + V_m} \quad (\text{Equation 2})$$

205 Where V_{i0} is the initial volume of ice with air (%) and V_m the initial volume of the unfrozen
206 matrix with air (%). The mass fraction of ice was then estimated with equation 3.

$$207 \quad X_i = \frac{\varphi_i \cdot \rho_i}{\rho_S} \quad (\text{Equation 3})$$

208 Where ρ_i is the volumetric mass density of ice (917 kg.m⁻³) and ρ_s the volumetric mass
209 density of a sorbet made with a solution containing 25%wt of sucrose in water (1100 kg.m⁻³).

210 **2.4.Cryo-SEM analyses**

211 Cryo-SEM measurements were carried out in an external laboratory equipped with scanning
212 electron microscopy (Electron Microscopy Facility, IBPS, Paris, France). The fresh sorbet
213 was taken in a pre-cooled plastic straw and then soaked in liquid nitrogen. The straw was cut
214 and a fragment of sorbet was cryofractured. Fractured surfaces were observed with cryo-SEM
215 (GeminiSEM 500, Zeiss) at -120 °C and 1.6x10⁻⁴ Pa, with an accelerating voltage of 3.00 kV
216 or 0.790 kV and a magnification from x13 to x10 000. The pixel resolution was between 11
217 nm and 9µm depending on the magnification. Manual segmentation and separation of
218 particles (i.e. ice crystals or air bubbles) were performed with Avizo 2019.1®. Equivalent
219 diameters of particles were obtained with equation 4. In 2D geometry, it is defined as the
220 diameter of a disk of same area than the particle.

$$221 \quad d_s = \sqrt{\frac{4*S}{\pi}} \quad (\text{Equation 4})$$

222 Where S is the surface of the particle.

223 **2.5.FBRM analyses**

224 The protocol for Focused Beam Reflectance Measurement analysis developed by Haddad
225 Amamou et al. (2010), used by Arellano et al. (2011) and Arellano et al. (2012) was
226 reproduced. The probe Lasentec® FBRM S400-8 (Mettler Toledo, Columbus, USA) was
227 used; it is made of stainless steel and has an external diameter of 9.5 mm and a length of
228 120 mm. The probe generates a focused laser beam (780 nm) which rotates at a high rate of
229 speed (about 2 m/s) and is projected inside the sample through a sapphire window. When a
230 particle is intersected by the laser beam, it reflects the laser light for the duration of its scan.
231 The time period of reflection is detected by the FBRM probe. By considering the tangential
232 speed of the laser beam, a corresponding chord length of the particle is calculated.

233 The probe was inserted into the batch freezer at about 4 cm from the wall with an inclination
234 of 45°. The temperature of the product being frozen is directly related to the amount of ice
235 formed thanks to the equilibrium liquidus curve of a sucrose sorbet; a calibrated thermocouple

236 was then inserted near the FBRM probe. FBRM measurement was then analyzed for a given
237 quantity of ice.

238 Data were collected with iC FBRM™ software (Mettler Toledo). Every second, the counts
239 number n_i was recorded for each selected size class i of chord length c_i . A Mean Chord
240 Length (MCL) was calculated (equation 5); this was equivalent to a mean Sauter diameter
241 (i.e. the mean diameter of spheres having the same ratio volume to surface than the particles).

$$242 \quad MCL = \frac{\sum n_i c_i^3}{\sum n_i c_i^2} \text{ (Equation 5)}$$

243 **2.6. Statistics**

244 Three samples were analyzed for X-ray micro-CT and FBRM analyzes. A batch of sorbet was
245 carried out per sample to ensure a reproducible sampling of the sorbet, at the same
246 temperature corresponding to the same amount of ice. For every parameter (equivalent
247 diameters, volume fractions, mean chord length), analysis of variance was applied to
248 determine significant differences ($p < 0.05$).

249 Cryo-SEM analyzes were carried out in an external laboratory specialized in microscopic
250 studies, in order to confirm the microtomographic results. As a consequence, only one sample
251 was analyzed with cryo-SEM. The entire cryo-fractured area was imaged so as to visualize a
252 sufficient number of objects for image analysis. .

253 **3. Results and discussion**

254 **3.1. Influence of stabilizers on air bubbles size and quantity**

255 3D visualizations of air bubbles in the samples obtained using micro-CT are shown in Figure
256 1; they give qualitative information about spatial distribution and number of air bubbles.
257 Concerning the unstabilized sample (Figure 1 (a)), there was a small quantity of air bubbles,
258 they were heterogeneous in terms of size and shape and randomly distributed in the 3D
259 volume. Similar air bubbles number and distribution were obtained with the sorbet containing
260 0.135% of CMC (Figure 1 (b)) whereas in the sorbet containing 0.3% of CMC, a higher
261 proportion of small bubbles was observed compared to the control (Figure 1 (c)). There were
262 more air bubbles in the LBG sample but their size distribution seemed still heterogeneous
263 (Figure 1 (d)) compared to the control sample. Concerning the HPMC sorbet (Figure 1 (e)),

264 air bubbles were numerous; they were small and uniformly distributed throughout the volume
265 of the cube.

266 A cryo-SEM raw image of an unstabilized sample is reported in Figure 2 (a). Only one or two
267 air bubbles were distinguished in these samples when using this technique, it was therefore
268 not possible to segment the air phase in these cases. The same observations were made with
269 samples containing LBG or CMC (data not shown). The low number of air bubbles in these
270 samples highlighted previously with micro-CT compared to the HPMC sorbet may explain
271 that there was no air bubble in the fractured planes visualized in cryo-SEM. Then, unlike with
272 micro-CT, the distinction of particles using cryo-SEM is not based on a difference in gray
273 level. It was therefore possible that some air bubbles were mistaken for ice crystals. A cryo-
274 SEM raw image of a sorbet containing HMPC is shown in Figure 2 (b). A large quantity of air
275 bubbles was observable, which is in accordance with the large quantity of air bubbles
276 observed with micro-CT analyzes. The segmentation and separation of air bubbles in the
277 HPMC sample (Figure 2 (c)) confirmed the observation made with micro-CT: air bubbles
278 were small and numerous even if they seemed less uniformly distributed than with micro-CT
279 visualization.

280 The size distributions of air bubbles according to the composition of the sorbet mix and the
281 analysis technique are shown in Figure 3. The results of micro-CT data treatment are
282 illustrated in Figure 3 (a). First, CMC added at 0.135% had no effect on the size distribution
283 of the air bubbles compared to the control sorbet: 75% of the air bubble are lower than 150
284 μm and the higher class reached up to 250-300 μm . HPMC and LBG presented the same size
285 distribution and ,compared to the control sample, they revealed a significantly higher
286 proportion of bubbles between 50 μm and 100 μm and more than 90% are lower than 150
287 μm . Concerning the 0.3% CMC sorbet; it contained significantly more bubbles of size less
288 than 50 μm and lower proportions of bubbles in size classes larger than 100 μm . The bubble
289 size distributions obtained with micro-CT and with cryo-SEM for the HPMC sorbet are
290 compared in Figure 3 (b). The trends were the same, which tended to confirm the validity of
291 micro-CT measurements and image processing.

292 Table 2 combines the quantitative results for air bubbles after micro-CT and cryo-SEM image
293 analyses. First, the air volume fraction was significantly higher in the HPMC sorbet (about
294 19%) than in the other sorbets (between 5% and 9%). The number of air bubbles was also
295 significantly higher with HPMC and to a lesser extent with LBG compared to the other

296 sorbets. It was therefore expected that the air bubbles were smaller in both LBG and HPMC
 297 sorbets than in the control sorbet. The mean bubble size was effectively smaller in the HPMC
 298 sorbet (about 70 μm) and in the LBG sorbet (about 85 μm) than in the control sorbet (about
 299 120 μm). Despite the low number of air bubbles observed in cryo-SEM in the HPMC sorbet,
 300 the size of air bubbles using this technique was in the same order of magnitude than the
 301 micro-CT values. HPMC is a surface-active polysaccharide, macromolecules adsorb to the
 302 gas/liquid interfaces and stabilizes the air bubbles (Clarke, 2012; Sarkar, 1984); the HPMC
 303 sorbet was then expected to contain a higher amount of air and smaller bubbles than the other
 304 sorbets. In the case of LBG, it could contain a small amount of proteins which would have
 305 interfacial properties and thus stabilize small bubbles; indeed the degree of purity of LBG was
 306 not mentioned by the supplier.

Table 2 : Air bubbles quantitative data obtained with micro-CT and cryo-SEM

	Unstabilized	HPMC	LBG	CMC 0.135%	CMC 0.3%	
X-Ray Micro-CT	Volume fraction (%)	5.6 \pm 0.7a	19.1 \pm 3.0b	9.0 \pm 2.6a	7.3 \pm 3.1a	5.3 \pm 1.4a
	Number of particles	307 \pm 74c	12 823 \pm 3 046d	1 576 \pm 359e	254 \pm 95c	375 \pm 87c
	Mean equivalent diameter (μm)	123 \pm 13f	71 \pm 6g	86 \pm 11g	108 \pm 34f,g	75 \pm 11g
	Median equivalent diameter (μm)	105 \pm 12f	67 \pm 10g	67 \pm 11g	69 \pm 24f,g	50 \pm 9g
Cryo- SEM	Number of particles analyzed		162			
	Mean equivalent diameter (μm)	–	66	–	–	–
	Median equivalent diameter (μm)	–	59	–	–	–

Different lower case letters indicate significant differences between values, $p < 0.05$.

307 CMC added at 0.135% to a sorbet mix did not seem to have any effect on the volume of air
 308 nor on the number of air bubbles; bubble size (mean and median) was not affected either.
 309 Before freezing, this mix was 8 times more viscous than the control mix and all stabilized
 310 mixes were isoviscous (Table 1). Therefore, this increase in viscosity was not enough to
 311 influence the aeration in the sorbet.

312 Added at 0.3%, CMC decreased the mean size of air bubbles as much as HPMC and LBG
 313 (75 μm) compared to the control (120 μm), without affecting the volume fraction of air or the
 314 number of bubbles. As expected when observing the size distributions of air bubbles (Figure

315 3), the median equivalent diameter was significantly smaller with 0.3% CMC sorbet than in
316 the control sample, indicating that CMC modified the size distribution with an higher
317 proportion of small bubbles. Before freezing, the 0.3% CMC mix was about 16 times more
318 viscous than the control mix and 2 times more viscous than the other stabilized mixes (Table
319 1). Such an increase in viscosity did not affect the amount of air or the quantity of bubbles but
320 could have affected their size distribution. This confirmed the ability of a viscous matrix to
321 slow down the coalescence of small air bubbles (Arbuckle, 1986; Clarke, 2012; Marshall et
322 al., 2003).

323 **3.2. Influence of stabilizers on ice crystals size and quantity**

324 **3.2.1. Analysis of fresh sorbets directly after freezing**

325 Results of micro-CT image processing of the ice phase are shown in Figure 4. Ice crystals are
326 individually color rendered by imaging processing. They appeared small and numerous
327 whatever the composition of the sorbet and no difference in ice crystal size or quantity was
328 founded between the samples at this stage of the analysis. Visual observation of micro-CT
329 images was therefore not sufficient to establish an eventual effect of stabilizers on the size and
330 morphology of ice crystals.

331 A cryo-SEM image of an unstabilized sample after manual segmentation and separation of ice
332 crystals is reported in Figure 5 (a). Similar images were obtained with samples containing
333 CMC (data not shown). An image of a HPMC sorbet after manual segmentation and
334 separation of ice crystals is reported in Figure 5 (b). The large presence of air bubbles made
335 the distinction of ice crystals difficult and the ice crystals partially covered by air bubbles
336 were excluded from the analysis. Finally, a small amount of crystals was analyzed in the
337 HPMC sample using cryo-SEM images.

338 Distributions of ice crystal sizes according to the imaging technique are shown in Figure 6.
339 Regarding the distribution obtained with micro-CT (Figure 6 (a)), it appeared that except for
340 the HPMC sorbet, all sorbets showed nearly the same distribution of ice crystals sizes. This
341 distribution seemed to follow a normal law with a majority of crystals between 50 and 70 μm .
342 Concerning the HPMC sorbet, more than 60% of crystals were lower than 50 μm , this could
343 suggest that HPMC prevents the growth of ice crystals during freezing. The same tendencies
344 were obtained using cryo-SEM (Figure 6 (b)).

345 Quantitative data concerning ice crystals in the different sorbet formulations observed in
 346 micro-CT and in cryo-SEM are given in Table 3. First, the mass fraction of ice calculated
 347 with micro-CT data was about 48% whatever the composition of the sorbet mixes, except for
 348 the HPMC which was slightly lower (about 43%). The ice mass fraction of a frozen sucrose
 349 solution at -6 °C given by the liquidus curve of the solution is estimated at 45% (Cerecero
 350 Enriquez, 2003). Therefore, in the conditions of the present study, stabilizers would have only
 351 a small influence on the quantity of ice produced during the freezing of a sorbet, regardless of
 352 the stabilizer concentration and thus of the initial apparent viscosity of the sorbet mix. This
 353 result is consistent with the literature; Herrera et al. (2007) found that 0.5% of LBG added to a
 354 20% sucrose solution did not significantly modify the percentage of formed ice at -7 °C or at
 355 -15 °C.

356 Micro-CT analysis showed that there were significantly more ice crystals in the HPMC sorbet
 357 than in the others (about 120000 and 70000 respectively). Therefore it was expected that the
 358 mean size of ice crystals was significantly reduced by the presence of HPMC but not by the
 359 other stabilizers. Finally, it was found that the HPMC sorbet contained crystals of about
 360 45 µm whereas all the others (control, LBG and CMC) were composed of crystals of about 65
 361 µm. Results about CMC were consistent with the literature ; Flores and Goff (1999) also
 362 concluded that CMC had no effect on the size of ice crystals when added at 0.26% to a 26%
 363 sucrose mix,.

364 Trends observed with micro-CT were also found with cryo-SEM. The mean sizes obtained
 365 were of the same order of magnitude and the value obtained with the HPMC sample was
 366 smaller than for the other samples. This allowed validating the micro-CT analysis, from
 367 sampling to image processing.

Table 3 : Ice crystals quantitative data obtained with micro-CT and cryo-SEM

		Unstabilized	HPMC	LBG	CMC 0.135%	CMC 0.3%
X-Ray Micro- CT	Mass fraction (%)	48.3±2.1a	43.0±1.1b	49.4±0.1a	46.0±2.5a,b	47.1±3.4a,b
	Number of particles	77 935±1826c	117 808±1 1886d	75 496±998c	68 775±4 812c	67 645±1 0562c
	Mean equivalent diameter (µm)	62.8±1.4e	45.6±2.8f	62.4±0.8e	64.2±1.5e	65.9±4.3e
Cryo- SEM	Number of particles analyzed	142	122	118	112	
	Mean equivalent diameter (µm)	56.5	50.8	54.8	59.7	—

Different lower case letters indicate significant differences between values, $p < 0.05$.

368 Before freezing, HPMC, LBG and 0.135% CMC mixes were about 8 times more viscous than
369 the control mix (Table 1) whereas LBG and 0.135% CMC sorbets contained crystals of nearly
370 the same size as the control sorbet (about 65 μm). This result shows that the viscosity at the
371 start of the process would not be the key parameter in controlling the ice crystal size. This
372 hypothesis tends to be confirmed comparing the crystals size in the 0.3% CMC sorbet to that
373 of the control sample: the crystals sizes are similar whereas the viscosity of the mix was 16
374 times higher (Table 1).

375 HPMC was the only hydrocolloid which increased significantly the amount of air in the sorbet
376 while decreasing the ice crystal size and increasing their quantity. These results raised the
377 question of the link between the influence of HPMC on quantity and size of ice crystals and
378 its surfactant properties. Air bubbles could be expected to insulate the freezing mix since the
379 thermal conductivity of air is much lower than that of water and ice. In this case, it would
380 theoretically extend the freezing time and thus led to the formation of larger ice crystals.
381 However, Thomas (1981) explained that a large amount of air would reduce ice crystal sizes
382 by mechanical hindrance. Clarke (2012) added that air bubbles could help to keep the ice
383 crystals separated and therefore to reduce accretion. Flores and Goff (1999) also noticed that
384 sorbets with higher amounts of air contained smaller crystals. The authors concluded that air
385 bubbles would act as a physical barrier during freezing by reducing collisions between
386 crystals and stretching the unfrozen matrix around them. Hernández Parra et al. (2018) also
387 observed that industrial sorbets (containing a mixture of HPMC, LBG and guar gum) with
388 higher overruns contained smaller crystals.

389 HPMC, LBG and 0.3 % CMC sorbets contained air bubbles of the same size, whereas the size
390 of ice crystals was only decreased in the presence of HPMC that gave the higher volume
391 fraction of air. This seems to indicate that the quantity of air is the key parameter in
392 controlling ice crystal size rather than the bubble size.

393 **3.2.2. Dynamic analysis of crystallization**

394 FBRM measurements were carried out continuously during the crystallization and coupled
395 with a continuous temperature recording. The ice distribution was specifically analyzed and
396 the mean chord length was calculated at three different temperatures : -2.5 $^{\circ}\text{C}$, -3.5 $^{\circ}\text{C}$ and
397 -4 $^{\circ}\text{C}$, corresponding respectively to approximately 10%wt, 30%wt and 35%wt of ice
398 according to the liquidus curve of a 25%wt sucrose solution (Cerecero Enriquez, 2003). When
399 the quantity of ice became too large, the sorbet escaped from the freezer and the signal from

400 the FBRM probe saturated; data were then no longer exploitable. Therefore it was not
401 possible to analyze sorbet at -6 °C with this technique, in contrast to micro-CT and cryo-SEM
402 analyses. Results obtained with the dynamic analysis of the crystallization of sorbets are
403 shown in Figure 7.

404 At -2.5 °C, the mean chord length was nearly the same (about 60 to 75 µm) whatever the
405 samples. This could indicate that the beginning of the crystallization and in particular the
406 nucleation was not affected by the presence of stabilizers used in this study.

407 Concerning the control sample, data recorded at -3.5 °C and -4 °C showed a significant
408 increase in the mean chord length measured (more than 150 µm and 200 µm respectively).
409 Indeed, above -2.5 °C, it was visually noticed that the unstabilized sorbet froze in the form of
410 large clusters of ice crystals while the other sorbets were much more homogeneous and
411 smooth. This could be related to the increase in the viscosity of the unfrozen residual solution
412 in the presence of stabilizer; in fact, this solution which surrounds the crystals could limit
413 their aggregation. Finally, it was difficult to follow the crystallization in the control sample
414 with the FBRM probe which was probably analyzing the entire clusters rather than individual
415 crystals. Therefore it will be difficult to compare the control with the other sorbets at
416 temperatures above -2.5 °C and these results will not be discussed further.

417 LBG and CMC sorbets showed an increase in the mean chord length during the freezing
418 process: from nearly 65µm at -2.5°C to nearly 100 µm at -3,5 °C and -4 °C. Furthermore there
419 was no significant difference of mean chord length at -4 °C between these samples (mean
420 value about 110 µm). This could indicate that under these conditions, crystals can grow in the
421 presence of LBG and CMC. Concerning the HPMC sorbet, there was no significant change in
422 the mean chord length during freezing (from 75 µm to 80 µm). At -4 °C, the mean chord
423 length was significantly smaller in the HPMC sorbet (about 80 µm) than in the other
424 stabilized samples. This result confirmed that under the conditions of the present study, the
425 growth of ice crystals was prevented during freezing in the presence of HPMC. Finally,
426 results seemed to be in agreement with the micro-CT and cryo-SEM data. However, all the
427 mean chord lengths obtained with FBRM was higher than the equivalent diameters
428 determined with micro-CT and cryo-SEM. This was probably due to the measurement mode
429 of the FBRM probe which measured chords lengths and not equivalent diameters.

430 **4. Conclusions and perspectives**

431 Sorbet mixes containing water, 25%wt of sucrose and HPMC, CMC or LBG as stabilizer
432 were frozen and sorbets were analyzed directly after their freezing by X-ray microtomography
433 and cryo-scanning electron microscopy. Image processing allowed obtaining quantitative
434 information about the ice and the air phase. The crystallization of water in sorbets was also
435 studied in real time during their freezing using an FBRM probe.

436 Comparing the results with the literature illustrated that, under the conditions of this study,
437 there would be no link between the rheological properties of mixes or unfrozen residual
438 solutions and ice crystals size. LBG and highly concentrated CMC decreased the size of air
439 bubbles while having no effect on the size of ice crystals neither on the mass fraction. HPMC
440 significantly increased the amount of air incorporated into the sorbet while reducing the size
441 of the bubbles. HPMC also significantly reduced the size of ice crystals, unlike the other
442 stabilizers which did not influence ice crystals size. The effect of HPMC on ice crystals size
443 seemed to be related to its surfactant properties which allowed incorporating a significantly
444 higher amount of air; air bubbles would act as a physical barrier and a mechanical hindrance
445 phenomenon would prevent crystal growth as confirmed with the analysis carried out with
446 FBRM. FBRM analyzes also showed that all the stabilizers tested would prevent the crystals
447 from agglomerating, this being probably related to their effect on the viscosity of the unfrozen
448 matrix.

449 Finally, this study provided a better understanding of the mechanisms of air incorporation and
450 crystallization in the presence of stabilizers. However, the specific mechanisms are not clearly
451 defined and other studies would be relevant to conclude. Studies of the surfactant properties
452 of HPMC and of the specific properties of LBG used in this study could be interesting to
453 better explain the results. The use of micro-CT, helpful to highlight the combine effect of air
454 bubbles in ice crystallization, could also be extended to the analysis of sorbets having more
455 complex compositions, in particular sorbets containing blends of stabilizers, in order to study
456 the possible synergistic effects of stabilizers on the crystallization of sorbets but also on air
457 incorporation.

458 **Funding**

459 This work was supported by the French Ministry of Higher Education, Research and
460 Innovation.

461 **References**

- 462 Arbuckle, W.S., (1986). *Ice Cream* (4th ed. ed). Springer, New York.
- 463 Arellano, M., Benkhelifa, H., Flick, D., Alvarez, G., (2012). Online ice crystal size measurements during
464 sorbet freezing by means of the focused beam reflectance measurement (FBRM) technology.
465 Influence of operating conditions. *Journal of Food Engineering*, 113(2), 351-359.
466 <https://doi.org/10.1016/j.jfoodeng.2012.05.016>
- 467 Arellano, M., Gonzalez, J.E., Alvarez, G., Benkhelifa, H., Flick, D., Leducq, D., (2011). Online ice crystal
468 size measurements by the focused beam reflectance method (FBRM) during sorbet freezing. *Procedia*
469 *Food Science*, 1, 1256-1264. <http://dx.doi.org/10.1016/j.profoo.2011.09.186>
- 470 Blond, G., (1988). Velocity of linear crystallization of ice in macromolecular systems. *Cryobiology*,
471 25(1), 61-66. [https://doi.org/10.1016/0011-2240\(88\)90021-1](https://doi.org/10.1016/0011-2240(88)90021-1)
- 472 Cerecero Enriquez, R., (2003). Etude des écoulements et des transferts thermiques lors de la
473 fabrication d'un sorbet à l'échelle du pilote et du laboratoire. Institut National Agronomique Paris
474 Grignon, Paris, p. 161.
- 475 Chang, Y., Hartel, R.W., (2002). Development of air cells in a batch ice cream freezer. *Journal of Food*
476 *Engineering*, 55(1), 71-78. [https://doi.org/10.1016/S0260-8774\(01\)00243-6](https://doi.org/10.1016/S0260-8774(01)00243-6)
- 477 Clarke, C., (2012). *The Science of Ice Cream* (2nd ed). RSCPublishing, Cambridge.
- 478 Doyle, J.P., Giannouli, P., Martin, E.J., Brooks, M., Morris, E.R., (2006). Effect of sugars, galactose
479 content and chainlength on freeze-thaw gelation of galactomannans. *Carbohydr. Polym.*, 64(3), 391-
480 401. <https://doi.org/10.1016/j.carbpol.2005.12.019>
- 481 Fernandez, P.P., Martino, M.N., Zaritzky, N.E., Guignon, B., Sanz, P.D., (2007). Effects of locust bean,
482 xanthan and guar gums on the ice crystals of a sucrose solution frozen at high pressure. *Food*
483 *Hydrocolloids*, 21(4), 507-515. <https://doi.org/10.1016/j.foodhyd.2006.05.010>
- 484 Flores, A.A., Goff, H.D., (1999). Ice crystal size distributions in dynamically frozen model solutions and
485 ice cream as affected by stabilizers. *Journal of Dairy Science*, 82, 1399-1407.
486 [https://doi.org/10.3168/jds.S0022-0302\(99\)75366-X](https://doi.org/10.3168/jds.S0022-0302(99)75366-X)
- 487 Goff, H.D., Caldwell, K.B., Stanley, D.W., Maurice, T.J., (1993). The influence of polysaccharides on the
488 glass-transition in frozen sucrose solutions and ice-cream. *Journal of Dairy Science*, 76(5), 1268-1277.
489 [https://doi.org/10.3168/jds.S0022-0302\(93\)77456-1](https://doi.org/10.3168/jds.S0022-0302(93)77456-1)
- 490 Goff, H.D., Ferdinando, D., Schorsch, C., (1999). Fluorescence microscopy to study galactomannan
491 structure in frozen sucrose and milk protein solutions. *Food Hydrocolloids*, 13(4), 353-362.
492 [https://doi.org/10.1016/S0268-005X\(99\)00017-X](https://doi.org/10.1016/S0268-005X(99)00017-X)

- 493 Goff, H.D., Hartel, R.W., (2013). *Ice cream* (7th ed. ed). Springer, New York.
- 494 Guo, E., Kazantsev, D., Mo, J., Bent, J., Van Dalen, G., Schuetz, P., Rockett, P., StJohn, D., Lee, P.D.,
495 (2018). Revealing the microstructural stability of a three-phase soft solid (ice cream) by 4D
496 synchrotron X-ray tomography. *Journal of Food Engineering*, 237, 204-214.
497 <https://doi.org/10.1016/j.jfoodeng.2018.05.027>
- 498 Guo, E., Zeng, G., Kazantsev, D., Rockett, P., Bent, J., Kirkland, M., Van Dalen, G., Eastwood, D.S.,
499 StJohn, D., Lee, P.D., (2017). Synchrotron X-ray tomographic quantification of microstructural
500 evolution in ice cream-a multi-phase soft solid. *RSC Advances*, 7(25), 15561-15573.
501 <https://doi.org/10.1039/c7ra00642j>
- 502 Haddad Amamou, A., Benkhelifa, H., Alvarez, G., Flick, D., (2010). Study of crystal size evolution by
503 focused-beam reflectance measurement during the freezing of sucrose/water solutions in a scraped-
504 surface heat exchanger. *Process Biochemistry*, 45(11), 1821-1825.
505 <http://dx.doi.org/10.1016/j.procbio.2010.04.001>
- 506 Hernández-Parra, O.D., Plana-Fattori, A., Alvarez, G., Ndoye, F.-T., Benkhelifa, H., Flick, D., (2018).
507 Modeling flow and heat transfer in a scraped surface heat exchanger during the production of
508 sorbet. *Journal of Food Engineering*, 221, 54-69. <https://doi.org/10.1016/j.jfoodeng.2017.09.027>
- 509 Hernández Parra, O.D., Ndoye, F.T., Benkhelifa, H., Flick, D., Alvarez, G., (2018). Effect of process
510 parameters on ice crystals and air bubbles size distributions of sorbets in a scraped surface heat
511 exchanger. *International Journal of Refrigeration*, 92, 225-234.
512 <https://doi.org/10.1016/j.ijrefrig.2018.02.013>
- 513 Herrera, M.L., M'Cann, J.I., Ferrero, C., Hagiwara, T., Zaritzky, N.E., Hartel, R.W., (2007). Thermal,
514 mechanical, and molecular relaxation properties of frozen sucrose and fructose solutions containing
515 hydrocolloids. *Food Biophysics*, 2(1), 20-28. <https://doi.org/10.1007/s11483-007-9025-8>
- 516 Kobayashi, R., Kimizuka, N., Suzuki, T., Watanabe, M., (2014). Effect of supercooled freezing methods
517 on ice structure observed by X-ray CT, *Refrigeration Science and Technology*, pp. 392-396.
- 518 Marshall, R.T., Arbuckle, W.S., (1996). *Ice cream* (5th ed. ed). Chapman & Hall, New York.
- 519 Marshall, R.T., Goff, H.D., Hartel, R.W., (2003). *Ice cream* (6th ed. ed). Springer, New York.
- 520 Masselot, V., Benkhelifa, H., Cuvelier, G., Bosc, V., (2020a). Rheological properties of stabilizers at low
521 temperatures in concentrated sucrose solutions. *Food Hydrocolloids*, 103, 105691.
522 <https://doi.org/10.1016/j.foodhyd.2020.105691>
- 523 Masselot, V., Bosc, V., Benkhelifa, H., (2020b). Analyzing the microstructure of a fresh sorbet with X-
524 ray micro-computed tomography: Sampling, acquisition, and image processing. *Journal of Food*
525 *Engineering*, 110347. <https://doi.org/10.1016/j.jfoodeng.2020.110347>
- 526 Mo, J., Groot, R.D., McCartney, G., Guo, E., Bent, J., van Dalen, G., Schuetz, P., Rockett, P., Lee, P.D.,
527 (2019). Ice crystal coarsening in ice cream during cooling: A comparison of theory and experiment.
528 *Crystals*, 9(6). <https://doi.org/10.3390/cryst9060321>
- 529 Mo, J., Guo, E., Graham McCartney, D., Eastwood, D.S., Bent, J., Van Dalen, G., Schuetz, P., Rockett,
530 P., Lee, P.D., (2018). Time-resolved tomographic quantification of the microstructural evolution of ice
531 cream. *Materials*, 11(10). <https://doi.org/10.3390/ma11102031>

532 Mousavi, R., Miri, T., Cox, P.W., Fryer, P.J., (2005). A Novel Technique for Ice Crystal Visualization in
533 Frozen Solids Using X-Ray Micro-Computed Tomography. *Journal of Food Science*, 70(7), 437-442.
534 <https://doi.org/10.1111/j.1365-2621.2005.tb11473.x>

535 Mousavi, R., Miri, T., Cox, P.W., Fryer, P.J., (2007). Imaging food freezing using X-ray
536 microtomography. *International Journal of Food Science and Technology*, 42(6), 714-727.
537 <https://doi.org/10.1111/j.1365-2621.2007.01514.x>

538 Muhr, A.H., Blanshard, J.M.V., (1986). Effect of polysaccharide stabilizers on the rate of growth of ice.
539 *Int. J. Food Sci. Tech.*, 21(6), 683-710. <https://doi.org/10.1111/ijfs1986216683>

540 Mulot, V., Fatou-Toutie, N., Benkhelifa, H., Pathier, D., Flick, D., (2019). Investigating the effect of
541 freezing operating conditions on microstructure of frozen minced beef using an innovative X-ray
542 micro-computed tomography method. *Journal of Food Engineering*, 262, 13-21.
543 <https://doi.org/10.1016/j.jfoodeng.2019.05.014>

544 Patmore, J.V., Goff, H.D., Fernandes, S., (2003). Cryo-gelation of galactomannans in ice cream model
545 systems. *Food Hydrocolloids*, 17(2), 161-169. [https://doi.org/10.1016/S0268-005X\(02\)00048-6](https://doi.org/10.1016/S0268-005X(02)00048-6)

546 Pinzer, B.R., Medebach, A., Limbach, H.J., Dubois, C., Stampanoni, M., Schneebeli, M., (2012). 3D-
547 characterization of three-phase systems using X-ray tomography: tracking the microstructural
548 evolution in ice cream. *Soft Matter*, 8(17), 4584-4594. <https://doi.org/10.1039/C2SM00034B>

549 Sarkar, N., (1984). Structural interpretation of the interfacial properties of aqueous solutions of
550 methylcellulose and hydroxypropyl methylcellulose. *Polymer*, 25(4), 481-486.
551 [https://doi.org/10.1016/0032-3861\(84\)90206-4](https://doi.org/10.1016/0032-3861(84)90206-4)

552 Stogo, M., (1998). *Ice cream and frozen desserts: a commercial guide to production and marketing*.
553 John Wiley & Sons, Hoboken.

554 Thomas, E.L., (1981). Structure and properties of ice cream emulsions. *Food Technol.*, 35(1), 41-48.

555 Thombare, N., Jha, U., Mishra, S., Siddiqui, M.Z., (2016). Guar gum as a promising starting material
556 for diverse applications: A review. *Int. J. Biol. Macromol.*, 88, 361-372.
557 <https://doi.org/10.1016/j.ijbiomac.2016.04.001>

558 Ullah, J., Takhar, P.S., Sablani, S.S., (2014). Effect of temperature fluctuations on ice-crystal growth in
559 frozen potatoes during storage. *LWT - Food Science and Technology*, 59(2P1), 1186-1190.
560 <https://doi.org/10.1016/j.lwt.2014.06.018>

561 Vicent, V., Ndoye, F.-T., Verboven, P., Nicolai, B., Alvarez, G., (2019). Effect of dynamic storage
562 temperatures on the microstructure of frozen carrot imaged using X-ray micro-CT. *Journal of Food
563 Engineering*, 246, 232-241. <https://doi.org/10.1016/j.jfoodeng.2018.11.015>

564 Vicent, V., Verboven, P., Ndoye, F.-T., Alvarez, G., Nicolai, B., (2017). A new method developed to
565 characterize the 3D microstructure of frozen apple using X-ray micro-CT. *Journal of Food Engineering*,
566 212, 154-164. <https://doi.org/10.1016/j.jfoodeng.2017.05.028>

567 Zhao, Y., Takhar, P.S., (2017). Micro X-ray computed tomography and image analysis of frozen
568 potatoes subjected to freeze-thaw cycles. *LWT - Food Science and Technology*, 79, 278-286.
569 <https://doi.org/10.1016/j.lwt.2017.01.051>

570

Figure 1

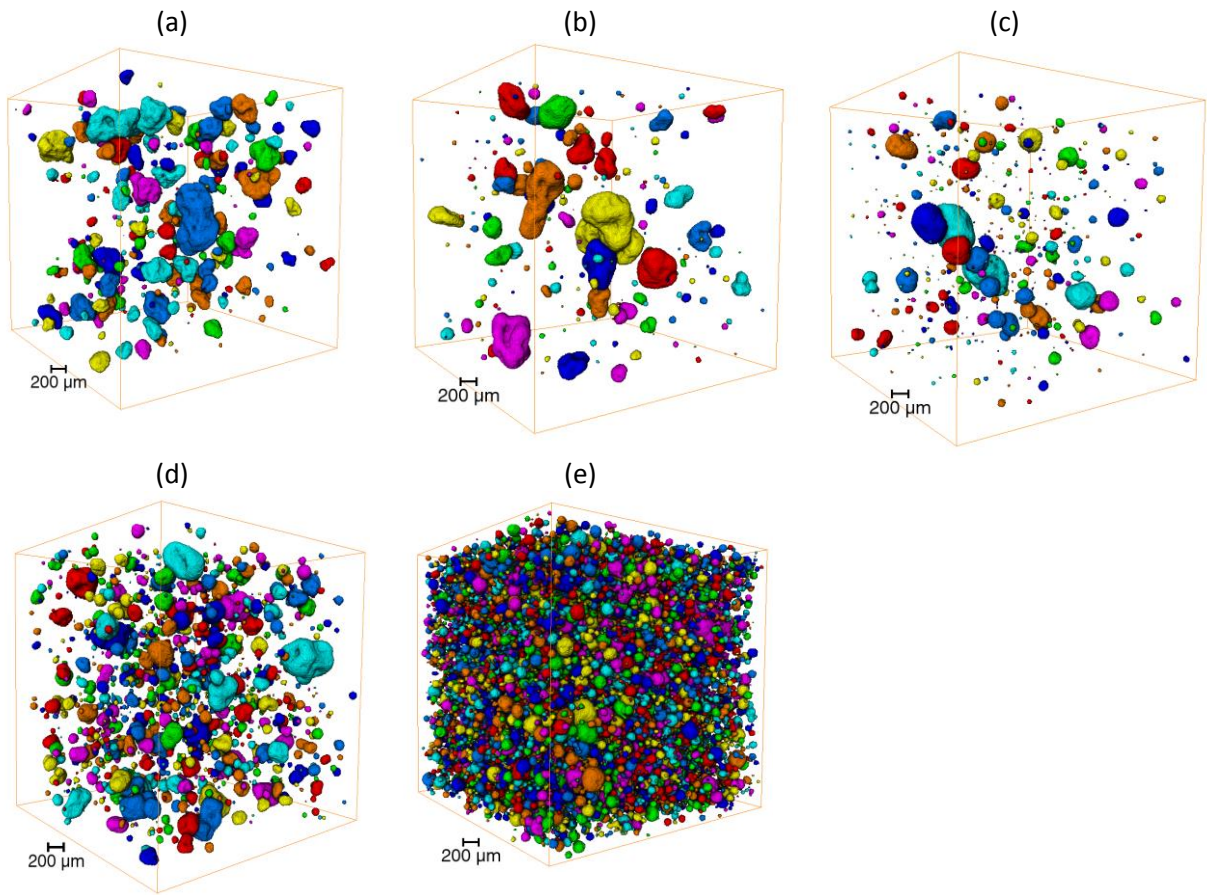


Figure 2

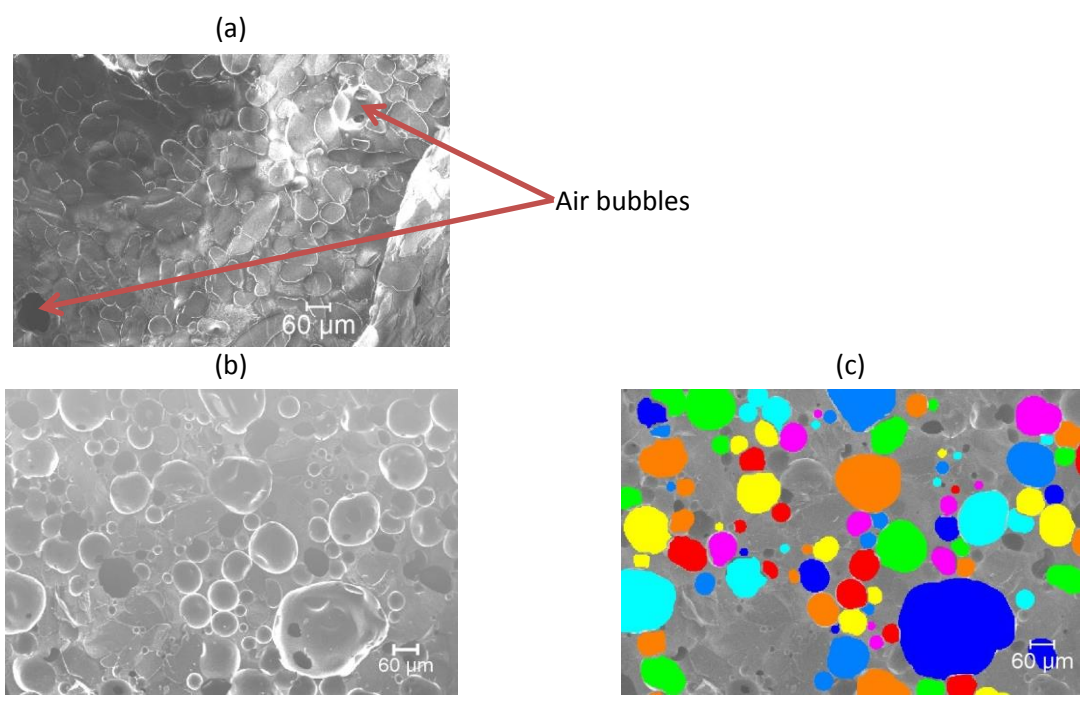


Figure 3

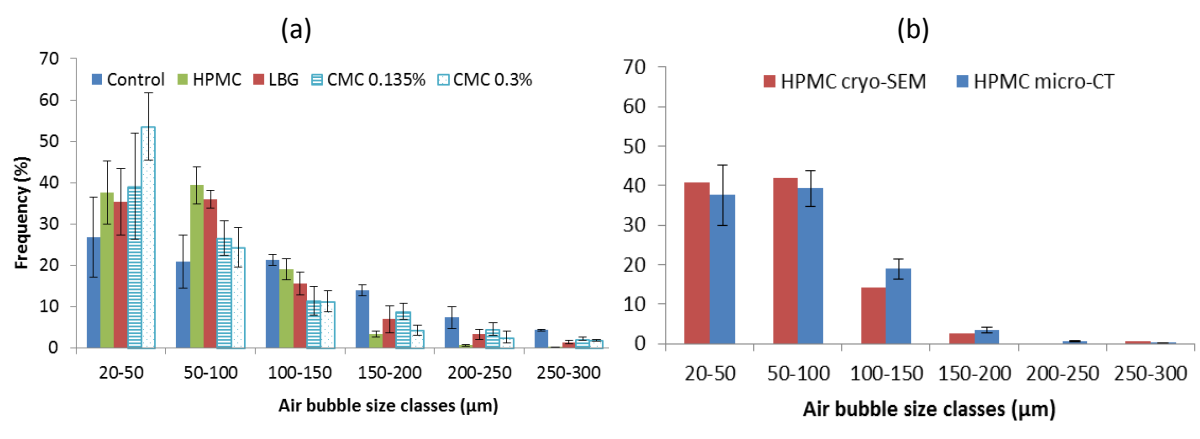


Figure 4

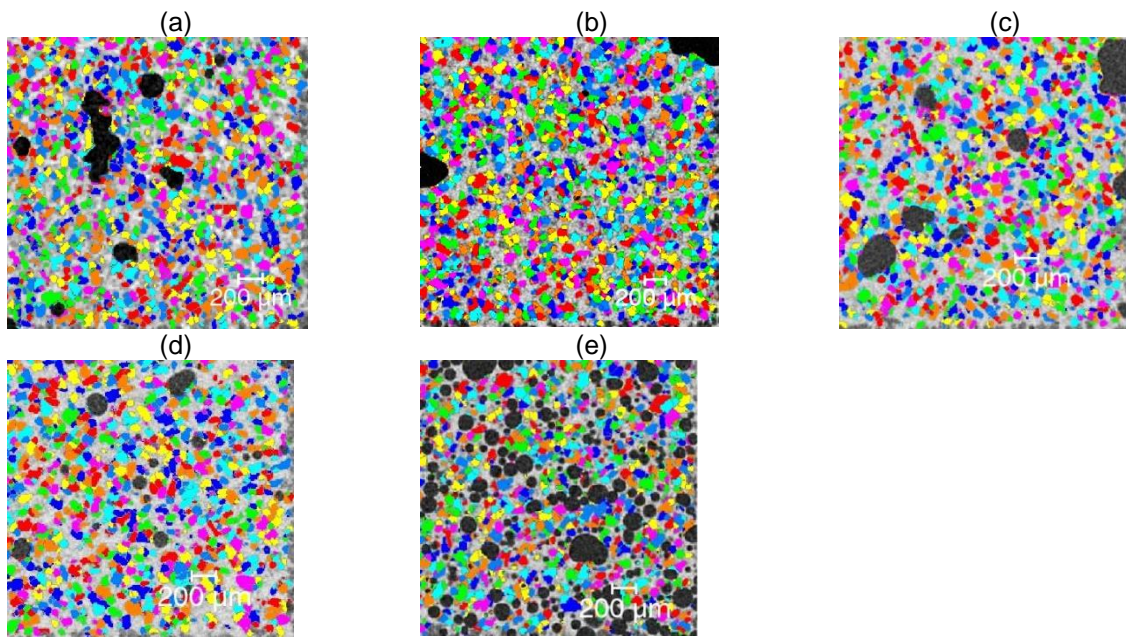


Figure 5

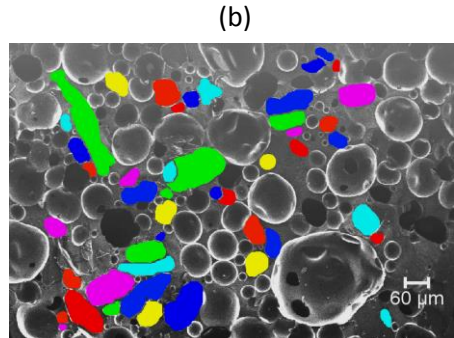
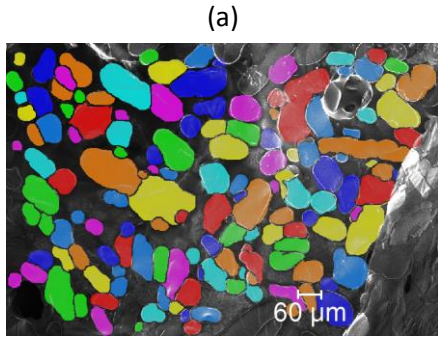


Figure 6

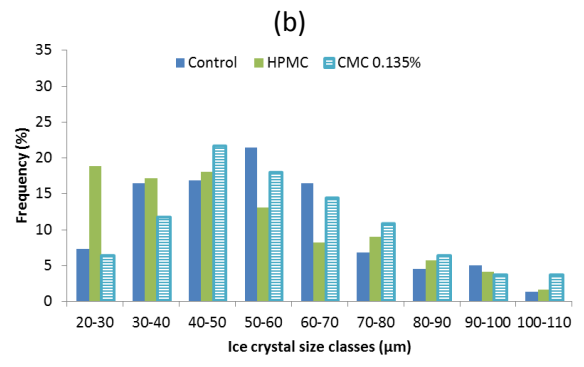
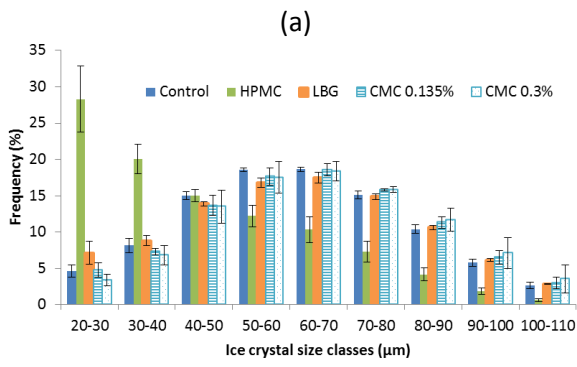


Figure 7

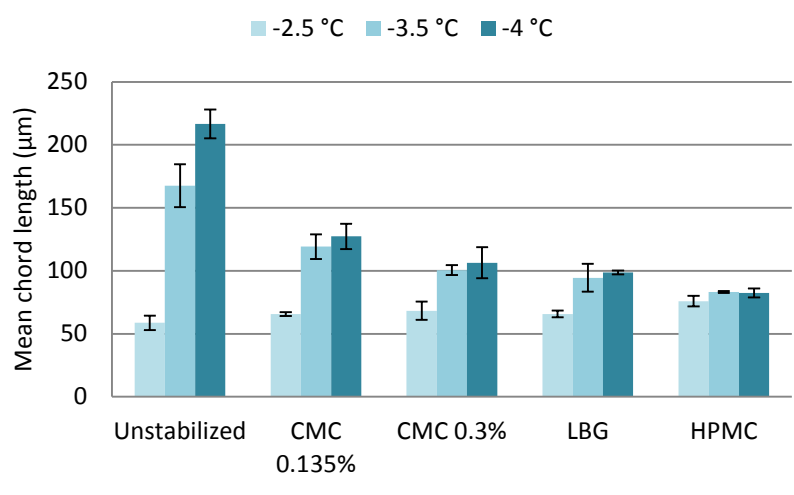


Figure 1: 3D representation of air bubbles

- (a) Control sample
- (b) CMC 0.135%
- (c) CMC 0.3%
- (d) LBG
- (e) HPMC

Figure 2: Cryo-SEM images

- (a) Raw image of unstabilized sample
- (b) Raw image of HPMC sample
- (c) Image obtained after segmentation separation of air bubbles for HPMC sample

Figure 3: Air bubble size distributions

- (a) Micro-CT
- (b) HPMC results: micro-CT versus cryo-SEM

Figure 4: Micro-CT image processing of the ice phase: Image obtained after segmentation and separation operations

- (a) Control sample
- (b) CMC 0.135%
- (c) CMC 0.3%
- (d) LBG
- (e) HPMC

Figure 5: Cryo-SEM images

- (a) Image obtained after segmentation and separation for unstabilized sample
- (b) Image obtained after segmentation and separation of ice crystals for HPMC sample

Figure 6: Ice crystal size distributions

- (a) Micro-CT
- (b) Cryo-SEM

Figure 7: Mean chord lengths of ice crystals obtained with FBRM experiments at three points in the freezing process

Declarations of interest: none.